PHYSICAL REVIEW B

CONDENSED MATTER

THIRD SERIES, VOLUME 44, NUMBER 20 15 NOVEMBER 1991-II

Electronic structure of antimony from density-functional calculations and angle-resolved photoemission

X. Gonze*
Unité PCPM, Université Catholique de Louvain, Place Croix du Sud, 1 B-1348 Louvain-la-Neuve, Belgium

R. Sporken, J. P. Vigneron, and R. Caudano
ISIS, Facultés Universitaires Notre-Dame de la Paix, Rue de Bruxelles 61, B-5000 Namur, Belgium

J. Ghijsen,† R. L. Johnson,‡ L. Ley,§ and H. W. Richter**
Max-Planck-Institut für Festkörperforschung, Heisenbergstrasse 1, Postfach 800665, D-7000 Stuttgart, Federal Republic of Germany
(Received 10 April 1991)

The electronic band structure of antimony was determined theoretically by an *ab initio* density-functional calculation and compared to an experimental study by angle-resolved ultraviolet photoemission spectroscopy. Most of the experimental results can be explained by direct transitions to free-electron states in a potential V_0, with good agreement between theory and experiment. Experimental quasiparticle energies for the three upper valence bands are given at Γ, T, U, W, L, and X. Some deviations, especially near T, are attributed to exchange-correlation self-energy effects. One experimentally observed band is tentatively identified as a surface state.

I. INTRODUCTION

Several theoretical and experimental investigations have been devoted to the study of the group-V semimetals arsenic, antimony, and bismuth for many years, mainly because of the interesting electrical transport properties of these materials.[1,2] Recently the band structures of bismuth[3] and arsenic[4] were studied experimentally with angle-resolved ultraviolet photoemission spectroscopy (ARUPS), and compared with theoretical band structures. Experiment and theory were in qualitative agreement, while quantitatively, some refinements and an increase in precision were needed. The study of bismuth focused on an interesting surface state in the spin-orbit gap. Due to the close similarity between the three group-V semimetals, it was interesting to perform a similar investigation for antimony.

We present here such a study of antimony band structure, measured by ARUPS and calculated using a state-of-the-art *ab initio* technique.[2] We also compare these results with the semiempirical calculation of Falicov and Lin[5] and Rose and Schuchardt.[6]

The paper starts with a presentation of the experimental work (Sec. II). Angle-resolved energy distribution curves for various off-normal angles were collected in two different planes parallel to ΓU and ΓW. Then (Sec. III), we briefly describe the *ab initio* theoretical method we used: *ab initio* pseudopotential, large basis of plane waves, density-functional formalism (DFF) treatment of the many-body problem. The interpretation of experimental data, using a free-electron final-state energy curve, is described in Sec. IV. In Sec. V, the results, in the form of band-structure curves along different lines, as well as precise values for six symmetry points, are presented. The discrepancies between experimental results and theory are analyzed.

II. EXPERIMENTAL WORK

Sb(111) samples were cleaved in ultrahigh vacuum (UHV) from single crystals whose orientation had been previously determined by x-ray diffraction. Low-energy electron diffraction (LEED) was performed on these samples and a sharp (1×1) pattern was obtained as usual for clean Sb(111) surfaces. This also allowed us to check the orientation of the samples with respect to the photon

beam. The samples were then transferred into the ARUPS spectrometer without breaking the UHV conditions. Since there was no facility for electron diffraction in the analysis chamber, the samples were aligned with respect to the manipulator axis, as determined by LEED in the preparation chamber.

Photoelectrons were excited by light from the TGM4 beamline at the storage ring BESSY. The photon energy was changed from 13 to 27 eV, which gives a monochromator resolution below 100 meV. A toroidal electrostatic analyzer[7] was used to measure angle-resolved energy distribution curves (EDC's) from the valence band. This analyzer allows us to measure EDC's for a full 180° in the plane of the incident light with an angular resolution of about 3° and an energy resolution of 70 meV in a single run. The angle of incidence was 45° and the light was linearly polarized in the plane of analysis. Two directions were measured, corresponding to the incident light along $\bar{\Gamma}\bar{U}$ and $\bar{\Gamma}\bar{W}$.

Since the measurement time is relatively short compared to the lifetime of the photon beam, and since quantitative analysis of the photoelectron intensities is not necessary for this work, no attempt was made to normalize the spectra with respect to the photon flux. The decrease of the photon flux was simply compensated by averaging an even number of scans recorded in alternating directions. The collection angles were calibrated in a separate run by introducing a series of slits at known positions between the sample and the analyzer, so that EDC's were obtained only for known collection angles.

Only data from samples with shiny, mirrorlike surfaces were used for this work. For samples with poor surface morphology due to a large number of steps, well-resolved valence-band EDC's could not be obtained. The cleanliness of the Sb(111) surfaces was checked directly from valence-band EDC's as well as from Sb(111) core-level spectra measured at 70-eV photon energy. The position of the Fermi level was determined from the emission of the metallic sample holder and from the top of the Sb valence-band spectrum.

III. BAND-STRUCTURE CALCULATIONS

Several empirical or semiempirical band structures of $A7$-structure antimony have already been published.[5,6,8] For our purpose, the comparison with the accurate semiempirical band-structure calculations of antimony by Falicov and Lin[5] and Rose and Schuchardt[6] is particularly interesting. Falicov and Lin use a semiempirical pseudopotential that they derive from other pseudopotentials adjusted for Ge and InSb. Rose and Schuchardt add a Heine-Abarenkov dielectric screening to a Golin-type pseudopotential, optimized to reproduce the experimental Fermi surface.

Contrary to those semiempirial previous studies, we have performed an *ab initio* electronic study: the only input was the experimental position of atoms.[9] We used the density-functional formalism[10] with the Ceperley-Adler expression for the exchange-correlation energy, as parametrized by Perdew and Zunger,[11] and the *ab initio* ionic pseudopotential of antimony, including spin-orbit coupling, found in the systematic work of Bachelet, Hamann, and Schlüter.[12] Although antimony is not as heavy as bismuth, it shows noticeable spin-orbit effects. In the context of the reciprocal-space formalism,[13] a large basis set of 411 plane waves was used, which generates sufficiently-well-converged electronic energies. The Bloch summations were performed over the irreducible part of the Brillouin zone, using a special-point scheme with 28 sampling points.[14] For more computational details, we refer the reader to a theoretical paper dealing with As, Sb, and Bi properties.[2]

The band structure generated in the framework of the density-functional technique, solving the Kohn-Sham equations, should not be exactly identical to the experimental quasiparticle band structure. The differences are mainly due to the neglect of the energy and state dependence of the self-energy by the use of a Kohn-Sham exchange-correlation potential. Usually, this strongly affects the band gap of semiconductors, whereas the valence bands of semiconductors, insulators, and metals are only slightly distorted.[15]

IV. ANALYSIS OF EXPERIMENTAL DATA

Figure 1 shows experimental EDC's for a photon energy $\hbar\omega = 17$ eV. The electrons are analyzed in the plane defined by the direction of the incoming light and the normal to the surface. For the spectra in Fig. 1, this plane is parallel to ΓU. These EDC's have been plotted for different collection angles θ (angle between the direction of observation and the normal to the surface) between 0° and 36°. The dispersion of the peaks is clearly visible in this figure. The peak marked by an arrow has no $\mathbf{k}_\perp$ dispersion and will be attributed later to a surface state.

Our analysis of experimental data follows the approach

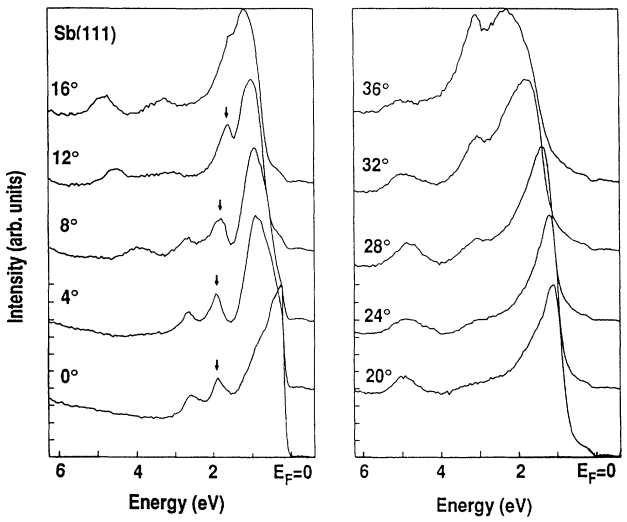

FIG. 1. Experimental valence-band energy distribution curves (EDC's) for Sb(111), collection angles ranging from 0° to 36°. The direction of the photons ($\hbar\omega = 17$ eV) is parallel to $\bar{\Gamma}\bar{U}$.

described in Ref. 16, graphically illustrated in Fig. 2. The electron in the initial state i (negative energy E_i with respect to the Fermi level, negative binding energy E_b with respect to the vacuum level E_{VL}), with momentum $\mathbf{k}$ ($\mathbf{k}=\mathbf{k}_{\parallel}+\mathbf{k}_{\perp}$, $\mathbf{k}_{\parallel}$ parallel to the normal of the surface), is excited by a photon of energy $\hbar\omega$ to a final state f (energy E_f with respect to the Fermi level E_F). Due to the nonconservation of $\mathbf{k}_{\perp}$ in photoemission experiments, the momentum and energy of the photoelectron in the initial state cannot be completely determined from the experiment without additional information. It is therefore assumed that the final state can be described by a free-electron dispersion energy in a so-called "inner potential" V_0. The photoelectron escapes the crystal and kinetic energy E_k. Usually, the value of the inner potential V_0 is negative. However, for the clarity of the discussion, we have shown it as a positive value in Fig. 2. This picture leads to the following relations:

$$\hbar^2 k_{\parallel}^2/2m = \sin^2\theta E_k \ , \tag{1}$$

$$\hbar\omega = E_c - E_b \ , \tag{2}$$

$$E_k = \hbar^2 k^2/2m + V_0 \ . \tag{3}$$

From our experimental data, we search for maxima in the EDC's and then obtain a set of values for E_b, $\mathbf{k}_{\perp}$, and $\mathbf{k}_{\parallel}$ from Eqs. (1)–(3). The measured photothreshold φ is 4 ± 0.2 eV. To determine $V_0+\varphi$, we first estimate it to be the difference between the theoretical bottom of the valence s band and the Fermi level (-12.6 eV). We then obtain the experimental band structure following the procedure outlined above and adjust $V_0+\varphi$ until the best agreement between theory and experiment is found for the whole spectrum. The retained value for $V_0+\varphi$ is -14 eV.

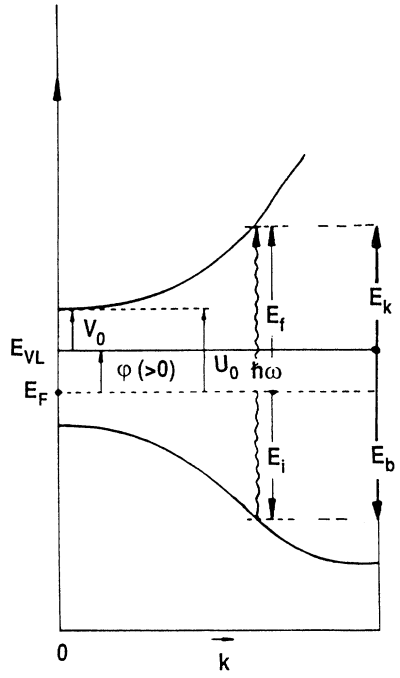

FIG. 2. Schematic drawing of the energy levels and energy differences appearing in our modelization of the electronic photoemission.

V. RESULTS

Figure 3 shows the experimental and theoretical band structure along selected symmetry lines. The usual notations for symmetry points and lines in the Brillouin zone have been used.[17] In particular, the ΓT direction is perpendicular to the surface, while TU and TWL are parallel to it.

A first set of experimental features can be unambiguously assigned to theoretical bands: the lowest band along TU, the three bands along UX, especially near X, the lowest band along $X\Gamma$, and the two upper ones near X along the same direction, the three bands along ΓT, the upper band along TL, and the shape of the two lowest bands along the same direction, although the positions of these latter ones are shifted.

Additional experimental dispersive features are observed along TWL and TU lines, while nondispersive ones are observed along TU, $X\Gamma$, and ΓT.

From the experimental data, we have extracted energies at symmetry points L, T, X, U, W, and Γ. These values are listed in Table I together with the corresponding theoretical values, and with the energies calculated by Falicov and Lin[5] and Rose and Schuchardt.[6] For most of the data, the agreement between theory and experiment is at least as good for our first-principles calculation as for the earlier semiempirical band structures.

Those values, which could not be matched to theoretical bands, are marked by an asterisk and will be discussed separately. The largest discrepancies are on the order of 0.4–0.5 eV. In a large zone near T, the two lowest experimental bands are found 0.4 eV below the corresponding theoretical bands. The magnitude of this shift decreases along $T\Gamma$, whereas it remains constant along TW.

The difference between our density-functional-theory calculation and the experiment is also shown in Table I. As already mentioned, the maximum difference is on the order of 0.5 eV, for an overall bandwidth of 6 eV. The values are regularly scattered around zero, and except for the two lowest bands near T, no other clear trend or simple distortion is present.

In the case of silicon, germanium, and diamond, the discrepancies between *ab initio* density-functional-theory calculations and ARUPS results have recently been investigated using the GW approximation to exchange-correlation self-energy.[15] As was already mentioned, the major discrepancy is the opening of the gap between valence and conduction bands for semiconductors. In addition, some distortion (of the order of 0.2 eV for Si and Ge, but up to 1.5 eV for diamond) affects the whole valence spectrum.

The fact that the two lowest bands at T seem to be influenced in the same manner by the self-energy can be related to the crystallographic structure of antimony: the

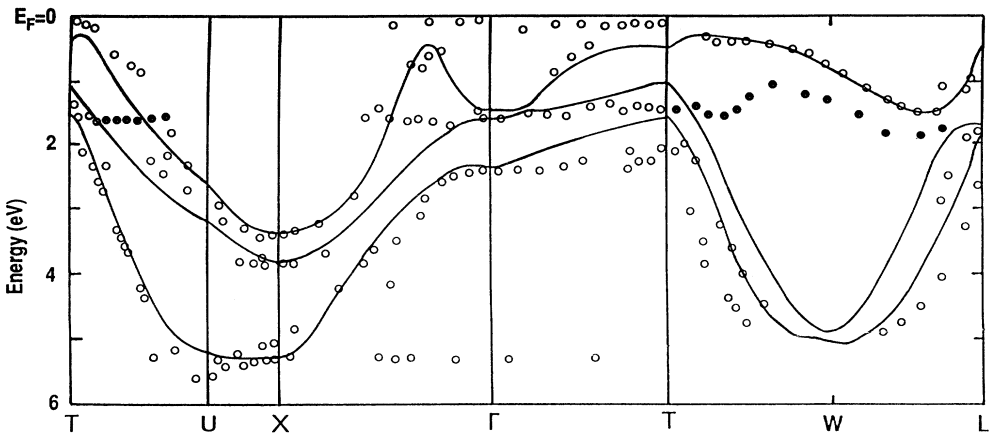

FIG. 3. Experimental electronic energies (circles) and theoretical band structure (lines) plotted along various lines in the Brillouin zone (see Ref. 17 for the notations). The solid circles are attributed to transitions from a surface state.

rhombohedral $A7$ structure. This structure can be obtained by a slight distortion of the simple cubic structure.[18] The two lowest valence p levels at the T point of $A7$-structure antimony come from the same level in the simple cubic geometry, and should therefore be affected similarly by the self-energy operator. On the other hand, the difference between the upper valence p level and the two lower p levels is not only due to the weak simple cu-

TABLE I. The experimental and theoretical energies at Γ, T, W, U, X, and L, with respect to the Fermi level. The three theoretical columns present the results of (1) this calculation, (2) the semiempirical pseudopotential calculation of Falicov and Lin (Ref. 5) (without spin-orbit coupling), and (3) the semiempirical screened pseudopotential calculation of Rose and Schuchardt (Ref. 6), with spin-orbit effects. The precision of the experimental values is indicated in parentheses. The last column presents the difference between the theoretical values (1) and the experimental ones, rounded to one significant digit. Asterisks indicate levels that cannot be matched with theoretical levels.

	Experiment (eV)	Theory (1)	(2)	(3)	Difference between experiment and theory (1)
Γ	−2.4(0.1)	−2.39	−1.47	−1.60	0.0
	−1.5(0.1)	−1.66	−1.28	−1.27	0.2
		−1.49	−1.28	−1.15	
	0.0*				
T	−2.1(0.2)	−1.56	−1.06	−1.08	−0.5
	−1.4(0.2)	−1.03	−1.06	−0.85	0.4
	−0.1(0.1)	−0.49	−0.44	−0.37	0.4
W	−4.8(0.2)	−4.98			0.2
		−4.82			0.0
	−1.3*(0.2)				
	−1.0(0.1)	−0.84			0.2
U	−5.6(0.2)	−5.33			−0.3
		−3.24			
	−2.6(0.2)	−2.63			0.0
X	−5.2(0.2)	−5.43	−4.79	−4.30	−0.2
	−3.9(0.1)	−3.89	−3.05	−2.94	0.0
	−3.4(0.1)	−3.46	−2.99	−2.74	0.1
L	−1.9(0.2)	−1.93	−1.52	−1.42	−0.0
		−1.80	−1.47	−1.32	
	−0.8(0.2)	−0.30	−0.35	−0.22	−0.5

bic to $A7$-structure crystal field, but also to the stronger spin-orbit interaction and simple cubic crystal field. This could explain the different influence of the self-energy operator on this level compared to the two lower p levels. A similar analysis of the crystallographic distortions has been proposed to explain the good agreement between experiment and theory for the semimetallic overlap of bismuth, while the general agreement for the energy levels around the Fermi energy is weaker for general levels at T and L for this element.[2,19] However, we have not tried to understand why the effect of the self-energy seems to be significantly smaller in other parts of the Brillouin zone in the case of antimony.

In addition to self-energy effects, the approximations made in the analysis of the experimental data could also influence the agreement between theory and experiment. In particular, we did not take any surface effect or electron-electron scattering into account.[20]

In some spectra, we have detected additional dispersive features. The first of these can be seen along TL, about 1 eV below the valence-band maximum. From the analysis of EDC's, we observed that this structure has no $\mathbf{k}_\perp$ dispersion. Since it is not predicted by the bulk band structure, and because of the absence of $\mathbf{k}_\perp$ dispersion, this state can be tentatively identified as a surface state on Sb(111) surface. Although we have no further proof for this interpretation, we note the striking similarity with a surface state observed by Jezequel *et al.*[3] on Bi.

The nondispersive feature along TU (i.e., along $\mathbf{k}_\perp$) is ascribed to the surface state just mentioned. The additional nondispersive features observed along $X\Gamma$ and ΓT could arise from indirect transitions because they coincide in energy with regions of high one-dimensional densities of states.

VI. CONCLUSION

The band structure of antimony—a group-V semimetal—has been investigated both experimentally and theoretically. The experimental technique was angle-resolved ultraviolet photoemission, using synchrotron radiation, and a state-of-the-art *ab initio* density-functional calculation was used for the theoretical investigation.

The theoretical and experimental results are consistent. We were able to determine experimental quasiparticle energies for the three upper valence p bands, along different lines in the Brillouin zone and in particular at six symmetry points, with an accuracy of 0.1–0.2 eV. The largest discrepancies between theory and experiment are of order 0.5 eV. We have discussed the possible sources of them, in particular the inadequate treatment of exchange-correlation self-energy in the framework of the density-functional formalism.

Some experimental features could not be ascribed to direct transitions from the bulk band structure. One of them could stem from a surface electronic state. Other structures are attributed to indirect transitions.

ACKNOWLEDGMENTS

We would like to thank Dr. J. Barth for his help with the experiment. We would also like to thank Professor J. P. Michenaud and Professor M. Cardona for support and encouragement. We are grateful to Professor M. Teter, Dr. C. Umrigar, and J. R. Morris for help or advice on this paper. Two of us (X.G. and R.S.) have received financial support from the National Fund for Scientific Research (FNRS-Belgium). This work was supported by FNRS-Belgium, by the Belgian Program on Interuniversity Attraction Poles initiated by the Belgian State–Prime Minister's Office–Science Policy Programming, and by the German Minister for Science and Technology under Grant No. 05490CAB. We also acknowledge the use of the Namur Scientific Computing Facility (Namur-SCF), a common project between the FNRS, IBM Belgium, and the Facultés Universitaires Notre Dame de la Paix (FUNDP).

*Present address: Laboratory of Atomic and Solid State Physics, Cornell University, Clark Hall, Ithaca NY 14853.

†Present address: Laboratoire Interdépartemental de Spectroscopie Electronique, Facultés Universitaires Notre-Dame de la Paix, rue de Bruxelles 61, B-5000 Namur, Belgium.

‡Present address: Institut für Experimentalphysik, Universität Hamburg, Luruperchaussee 149, D-2000 Hamburg 50, FRG.

§Present address: Institut für Technische Physik der Universität Erlangen–Nürnberg, Erwin Rommel Strasse 1, D-8520 Erlangen, FRG.

**Present address: Institut für Mikroelektronik Stuttgart, Allmandring 30, D-7000 Stuttgart 80, FRG.

[1]See M. S. Dresselhaus, J. Phys. Chem. Solids **33**, 3 (1971); J.-P. Issi, Aust. J. Phys. **32**, 585 (1979), and references therein.

[2]X. Gonze, J.-P. Michenaud, and J.-P. Vigneron, Phys. Rev. B **41**, 11 827 (1990).

[3]G. Jezequel, Y. Petroff, R. Pinchaux, and F. Yndurain, Phys. Rev. B **33**, 4352 (1986); see also D. Liebowitz, J. Muratore, Y. H. Kao, and N. J. Shevchik, Solid State Commun. **22**, 759 (1977).

[4]T. Takahashi, H. Ohsawa, N. Gunasekara, H. Ishii, T. Kinoshita, T. Sagawa, H. Kato, T. Miyahara, and K. Shindo, Phys. Scr. **36**, 187 (1987); H. Tokailin, T. Takahashi, T. Sagawa, and K. Shindo, Phys. Rev. B **30**, 765 (1984).

[5]L. M. Falicov and P. J. Lin, Phys. Rev. **141**, 562 (1966).

[6]J. Rose and R. Schuchardt, Phys. Status Solidi B **117**, 213 (1983).

[7]F. Toffoletto, R. C. G. Leckey, and J. D. Riley, Nucl. Instrum. Methods B **12**, 282 (1985).

[8]D. W. Bullet, Solid State Commun. **17**, 965 (1975); M. Iwamatsu, J. Phys. Soc. Jpn. **48**, 479 (1980); J. Robertson, Phys. Rev. B **28**, 4671 (1983).

[9]D. Schiferl and C. S. Barrett, J. Appl. Crystallogr. **2**, 30 (1969).

[10]P. Hohenberg and W. Kohn, Phys. Rev. **136**, B864 (1964); W. Kohn and L. J. Sham, *ibid.* **140**, A1133 (1965).

[11]D. M. Ceperley and B. J. Alder, Phys. Rev. Lett. **45**, 566 (1980); J. Perdew and A. Zunger, Phys. Rev. B **23**, 5048 (1981).

[12]G. B. Bachelet, D. R. Hamann, and M. Schlüter, Phys. Rev. B **26**, 4199 (1982).

[13]J. Ihm, A. Zunger, and M. L. Cohen, J. Phys. C **12**, 4409 (1979).
[14]H. J. Monkhorst and J. D. Pack, Phys. Rev. B **13**, 5188 (1976).
[15]M. S. Hybertsen and S. G. Louie, Phys. Rev. B **34**, 5390 (1986); R. W. Godby, M. Schlüter, and L. J. Sham, Phys. Rev. Lett. **56**, 2415 (1986); Phys. Rev. B **36**, 3497 (1987); **37**, 10 159 (1988).
[16]T.-C. Chiang, J. A. Knapp, M. Aono, and D. E. Eastman, Phys. Rev. B **21**, 3513 (1980); T.-C. Chiang and D. E. Eastman, *ibid.* **22**, 2940 (1980); see also Ref. 4 and references therein.
[17]M. H. Cohen, Phys. Rev. **121**, 387 (1961).
[18]R. I. Sharp and E. Warming, J. Phys. F **1**, 570 (1971).
[19]X. Gonze (unpublished).
[20]see T. Grandke, L. Ley, and Cardona, Phys. Rev. B **18**, 3847 (1978); T. Hora and M. Scheffler, *ibid.* **29**, 692 (1984).